15. Domingo, G., Itoga, R. S. & Kannewurf, C. R. Fundamental optical absorption in SnS_2 and $SnSe_2$. *Phys. Rev.* **143,** 536–541 (1966).
16. Shibata, T., Muranushi, Y., Miura, T. & Kishi, T. Electrical characterization of 2H-SnS_2 single crystals synthesized by the low temperature chemical vapor transport method. *J. Phys. Chem. Solids* **52,** 551–553 (1991).
17. Streetman, B. G. *Solid State Electronic Devices* 443 (Prentice-Hall, New Jersey, 1980).
18. McCandless, B. E., Mondal, A. & Birkmire, R. W. Galvanic deposition of cadmium sulfide thin films. *Sol. Energy Mater. Sol. Cells* **36,** 369–379 (1995).
19. Gan, F. Y. & Shih, I. Preparation of thin-film transistors with chemical bath deposited CdSe and CdS thin films. *IEEE Trans. Electron Devices* **49,** 15–18 (2002).
20. Ridley, B. A., Nivi, B. & Jacobson, J. M. All-inorganic field effect transistors fabricated by printing. *Science* **286,** 746–749 (1999).
21. Welsh, T. W. B. & Broderson, H. J. Anhydrous hydrazine. III. Anhydrous hydrazine as a solvent. *J. Am. Chem. Soc.* **37,** 816–824 (1915).
22. Eisenmann, B. & Hansa, J. Crystal structure of tetrapotassium hexaselenodistannate, $K_4Sn_2Se_6$. *Z. Kristallogr.* **203,** 299–300 (1993).
23. Pałosz, B., Steurer, W. & Schulz, H. Refinement of SnS_2 polytypes 2*H*, 4*H* and 18*R*. *Acta Crystallogr. B* **46,** 449–455 (1990).
24. Carey, P. G., Smith, P. M., Theiss, S. D. & Wickboldt, P. Polysilicon thin film transistors fabricated on low temperature plastic substrates. *J. Vac. Sci. Technol. A* **17,** 1946–1949 (1999).
25. Van der Veen, J. F. Ion beam crystallography of surfaces and interfaces. *Surf. Sci. Rep.* **5,** 199–287 (1985).
26. Dimitrakopoulos, C. D., Purushothaman, S., Kymissis, J., Callegari, A. & Shaw, J. M. Low-voltage organic transistors on plastic comprising high-dielectric constant gate insulators. *Science* **283,** 822–824 (1999).
27. Mitzi, D. B., Dimitrakopoulos, C. D. & Kosbar, L. L. Structurally tailored organic-inorganic perovskites: Optical properties and solution-processed channel materials for thin-film transistors. *Chem. Mater.* **13,** 3728–3740 (2001).
28. Duan, X. *et al.* High-performance thin-film transistors using semiconductor nanowires and nanoribbons. *Nature* **425,** 274–278 (2003).

Acknowledgements We thank C. Dimitrakopoulos for discussions, and D. Martinez, S. J. Chey, D. DiMilia, K. Fogel and T. Graham for technical assistance with the preparation of the substrates.

Competing interests statement The authors declare that they have no competing financial interests.

Correspondence and requests for materials should be addressed to D.B.M. (dmitzi@us.ibm.com).

A 'snowball Earth' climate triggered by continental break-up through changes in runoff

Yannick Donnadieu[1], Yves Goddéris[2], Gilles Ramstein[1], Anne Nédélec[2] & Joseph Meert[3]

[1]*Laboratoire des Sciences du Climat et de l'Environnement, CNRS-CEA, 91191, Gif sur Yvette, France*
[2]*Laboratoire des Mécanismes et Transferts en Géologie, UMR 5563, CNRS – Université Paul Sabatier – IRD, 31400, Toulouse, France*
[3]*Department of Geological Sciences, University of Florida, Gainesville, Florida 32611, USA*

Geological and palaeomagnetic studies indicate that ice sheets may have reached the Equator at the end of the Proterozoic eon, 800 to 550 million years ago[1,2], leading to the suggestion of a fully ice-covered 'snowball Earth'[3,4]. Climate model simulations indicate that such a snowball state for the Earth depends on anomalously low atmospheric carbon dioxide concentrations[5,6], in addition to the Sun being 6 per cent fainter than it is today. However, the mechanisms producing such low carbon dioxide concentrations remain controversial[7,8]. Here we assess the effect of the palaeogeographic changes preceding the Sturtian glacial period, 750 million years ago, on the long-term evolution of atmospheric carbon dioxide levels using the coupled climate[9]–geochemical[10] model GEOCLIM. In our simulation, the continental break-up of Rodinia leads to an increase in runoff and hence consumption of carbon dioxide through continental weathering that decreases atmospheric carbon dioxide concentrations by 1,320 p.p.m. This indicates that tectonic changes could have triggered a progressive transition from a 'greenhouse' to an 'icehouse' climate during the Neoproterozoic era. When we combine these results with the concomitant weathering effect of the voluminous basaltic traps erupted throughout the break-up of Rodinia[11], our simulation results in a snowball glaciation.

Long-term ($\geq 10^6$ yr) evolution of the partial pressure of atmospheric CO_2 (p_{CO_2}) is controlled by the relative importance of degassing through volcanic and mid-ocean-ridge processes and the consumption of CO_2 through continental silicate weathering[12]. Any long-term decrease in atmospheric CO_2 can be induced either by a decrease in solid Earth degassing rate, or by an increase in the weathering of continental surfaces. Little is known about the evolution of the degassing rate over the Neoproterozoic era, so linking the global Neoproterozoic cold climate to low degassing rate would be extremely speculative. On the other hand, the sink of CO_2 via continental silicate weathering depends on a variety of parameters, such as the air temperature, continental runoff[13], vegetation[14], and mechanical weathering[15]. The long-term evolution of some of these parameters can be evaluated within the particular context of the Neoproterozoic. The tectonic environment is indeed characterized by the dispersal of continental plates through the break-up of the Rodinia supercontinent between 800 and 700 Myr ago. This break-up may have had two major effects on the sink of CO_2 through continental silicate weathering. First, the break-up of Rodinia is heralded by, and accompanied by, the eruption of large basaltic provinces[11], resulting in an increase of the weatherability of the continental surface and consumption of atmospheric CO_2 on the 10^6-yr timescale[8,16]. More importantly, the break-up of a supercontinent into several smaller plates will result in an increase of precipitation and runoff over the continental masses, owing to an increase in the sources of moisture along continental borders. This process can boost continental silicate weathering and consume atmospheric CO_2. Hence, precise quantitative evaluation of changes in atmospheric p_{CO_2} due to palaeogeographic changes requires a sophisticated approach in which the weathering rates are spatially resolved.

We have interfaced a long-term global carbon cycle model to a coupled ocean–atmosphere model (GEOCLIM: 'geological timescales climate'). This approach allows us to account for the spatial variations (for example, longitude and latitude) of the climatic parameters used in the geochemical model to estimate continental weathering rates: runoff and temperature. We show here that the dispersal of the supercontinent results in an enhanced consumption of atmospheric CO_2, of the order of 1,320 p.p.m., and in a significant cooling of global temperatures (~8 °C). We further demonstrate that experiments accounting for the palaeogeographic effect on weathering rates together with the weathering of the large magmatic provinces produce conditions able to trigger a full snowball glaciation at 750 Myr ago.

The climate module of our coupled geochemical–climate model enabled us to address the following requirements. First, the model must explicitly simulate the hydrologic cycle, and second, the model must have a fast turnaround time. The coupled climate model CLIMBER-2 meets these requirements since, first, water fluxes are explicitly resolved, and second, the design of CLIMBER-2 results in a low computational cost, enabling very long simulations (a few thousand years). Briefly, the atmospheric module is a 2.5-dimensional statistical-dynamical model and has a resolution of 10° in latitude and approximately 51° in longitude. The ocean module describes the zonally averaged characteristics for the ocean realm with a latitudinal resolution of 2.5°. The CLIMBER-2 model is fully described in ref. 9, and successfully simulates the last glacial/interglacial cycle[17]; it has been used previously to investigate Neoproterozoic climates[18]. In order to determine the atmospheric CO_2 evolution, we use the geochemical COMBINE model[10], which is a box-model including the mathematical description of the global

biogeochemical cycles of carbon, phosphorus, alkalinity and oxygen (see Methods).

Figure 1a, b displays the two palaeogeographies used in this study; ~800 Myr ago (denoted SC, supercontinent configuration) and ~750 Myr ago (denoted DC, dispersed configuration), illustrating the dispersal of the supercontinent[19,20]. The numerical experiments are described in the Methods section. Changes in the continental distribution, from SC to DC, trigger a large decrease in atmospheric CO_2 levels from 1,830 p.p.m. to 510 p.p.m. for the standard runs with the present-day degassing rate (Fig. 2). The climate of the SC experiment at 1,830 p.p.m. is rather cold, given the reduction of 6% of the incoming solar radiation. Indeed, the mean global temperature is 10.8 °C (against 15 °C for the modern one). Nevertheless, regions of the Earth where temperatures are below the freezing point are mainly located over the polar oceans, and extend down to 60° latitude in both hemispheres (not shown). In contrast, in the DC climate simulation at 510 p.p.m., the freezing temperatures migrate towards mid-latitudes (40–45°; not shown) and the global mean temperature is reduced to only 2 °C. Figure 1a, b shows the spatially-resolved weathering rates at 1,830 p.p.m. for the SC and DC experiments.

The vast size of the supercontinent restricts the delivery of precipitation from oceanic moisture sources (Fig. 1c). Thus, the SC experiment yields the driest continental climates and the lowest weathering rates. In contrast, the DC experiment is characterized by high runoff and large weathering rates in the equatorial regions, because the continents are smaller and widely dispersed with numerous oceans and seaways available as moisture sources. Thus, the larger runoff of the DC simulation results in higher consumption of CO_2 through weathering, and forces the climate to cool until the silicate weathering rate reaches a value equal to the SC simulation (itself equal to the degassing rate). Thus, using a complex model and quantifying the effect of the break-up, we predict a marked reduction in the concentration of CO_2 in the atmosphere to a persistently low value in the range 400–630 p.p.m. on timescales of >10 Myr (Fig. 2). We also find that model-predicted DC CO_2 values are in the range of radiative forcings, resulting in the build-up of ice sheets at latitudes greater than 30° (refs 5, 6). These CO_2 concentrations are just above the threshold value required to trigger a snowball Earth with the GEOCLIM model, that is, 250 p.p.m. (Fig. 2). Although a dispersed continental configuration is a common feature for reconstructions at 750 Myr ago, the true palaeogeography evolves during the snowball intervals via normal continental motion. Additional experiments (not shown) were performed to determine the sensitivity of our results to alternative dispersed configuration (for instance, the position of Siberia in Fig. 10b of ref. 20). Those runs demonstrate that the break-up effect may be larger (the atmospheric CO_2 level could be as low as 420 p.p.m. instead of 510 p.p.m. for the standard runs).

Although these experiments show that continental break-up could prepare the Earth for full glaciation, all the events that occurred before and during the dislocation have not been accounted for. Indeed, the break-up of Rodinia was heralded by intense volcanism, including the emplacement of large basaltic provinces between 825 and 750 Myr ago[11]. Figure 3 illustrates the combined

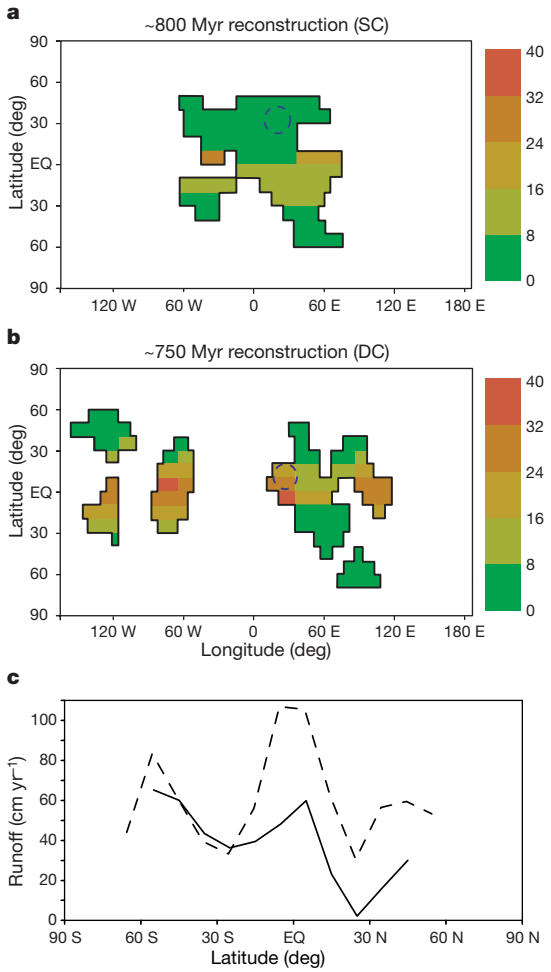

Figure 1 Palaeogeographies and hydrologic cycle. Weathering rates (10^4 mol km^{-2} yr^{-1}) simulated by the GEOCLIM model with a p_{CO_2} of 1,830 p.p.m.: **a**, for the continental reconstruction at ~800 Myr (denoted SC, supercontinent configuration), that is, before the Rodinia break-up, and **b**, for the continental reconstruction at ~750 Myr ago (denoted DC, dispersed configuration). Dashed circles, location of the basaltic provinces used for the runs including them. Accounting for the age error limits on these reconstructions, drift rates are between 13 and 8 cm yr^{-1}. Given that the break-up has been attributed to extensive volcanism and perhaps superplumes, these rates are quite consistent with the thermal regime proposed for the upper mantle. **c**, Annual mean zonal runoff (cm yr^{-1}) as simulated by the CLIMBER-2 model at a p_{CO_2} of 1,830 p.p.m. for the SC experiment (solid line) and for the DC experiment (dashed line).

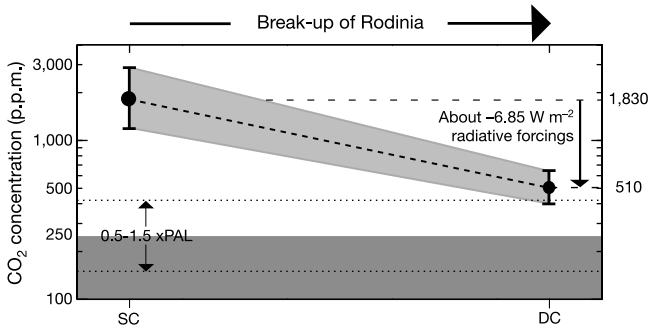

Figure 2 Effect of the Rodinia break-up on the greenhouse effect. Steady-state atmospheric CO_2 level achieved by the GEOCLIM model with the SC and DC reconstructions (Fig. 1). Vertical bars on the two data points denote the upper and the lower range of atmospheric CO_2 levels calculated using a 20% increase and a 20% decrease in degassing flux, respectively (see Methods). The horizontal dashed lines denote the exact CO_2 values reached by the model for the standard runs. The vertical arrow displays the change of the radiative forcing from direct CO_2 effects alone. The dark grey area shows the CO_2 levels required for a globally glaciated state in the 750-Myr-ago climate simulations we used here. The dotted lines denote the range of atmospheric CO_2 levels required for low-latitude glaciations as predicted by a diverse array of climate models[5,6] and are here for comparison with the threshold obtained by the GEOCLIM model. This range of CO_2 values is the consequence of several mechanisms that cannot be accounted for in a unique climate model. Among those mechanisms, ocean dynamics and sea-ice meltwater effects[18,30] (but also the inclusion of an ice-sheet model[5]) can have a profound effect on the position of the critical collapse point. PAL, present atmospheric level.

effect of the weathering of freshly erupted basaltic provinces and continental separation. This increase in continental weatherability does not initially result in a significant change in the CO_2 levels as the basaltic surfaces are located in the sub-tropics (see the dashed circle, Fig. 1a), the driest regions in our simulations (Fig. 1c). Subsequently, the southward drift of the Laurentia plate (and also of the basaltic surfaces, Fig. 1b) and the dispersion of the continents increase the weathering rates and lower the CO_2 levels past the threshold required to trigger a snowball Earth (that is, 250 p.p.m., Fig. 3). Hence, our model results provide an explanation for the severe cooling observed during the Sturtian interval, and highlight the complex interplay between atmospheric CO_2 content, the dispersal of Rodinia, and the silicate/basaltic weathering feedback as the primary causes of the 'greenhouse'–'icehouse' climate transition.

Although we are now able to explain the onset of a snowball glaciation during the Sturtian glacial period, it is worth seeing if this model can be applied to the younger Neoproterozoic glacial episodes. Of these, the Marinoan glaciation (~650–600 Myr ago) is thought to be global in extent[2] whereas the global nature of the younger glacial pulse (Varangian, ~580–565 Myr ago) is questioned[21–23]. Our present study indicates that dispersed continents positioned at low latitudes trigger reduction of global temperatures. Whether a continental configuration similar to the Sturtian one still applies to the younger glaciations is a matter of debate, primarily because of the lack of well-constrained palaeomagnetic data for the interval 700–580 Myr ago[19,20]. At present, the palaeogeographic models can be divided into two categories. The first is a supercontinent assembly, stretching from high southerly to low latitudes[20]. The second posits a situation very similar to the Sturtian epoch, with most continents in mid to low latitudes[24]. Although recent palaeomagnetic data and geochronologic data make a stronger case for the mid-to-low latitude configuration[24,25], these studies did not provide any global reconstructions that we could use in this investigation. However, we do note that if the low-to-mid latitude configuration is validated by further studies, then the similarities to the Sturtian situation suggest that our model may be applicable to the Marinoan event. We also note that the final trigger for this event was probably not basaltic surface weathering, but rather a transient methane-induced greenhouse, resulting in enhanced atmospheric CO_2 consumption[7]. This may explain the differences in the $\delta^{13}C$ excursions (both magnitude and timing) observed before both glaciations. Indeed, the available data suggest that the Sturtian glaciation was preceded by positive carbon isotopic values whereas the Marinoan glaciation was preceded by an impressive but gradual decline in $\delta^{13}C > 10‰$ (ref. 23).

The latest Varangian event (the Gaskiers glaciation) was attributed to a regionally extensive glaciation rather than to a snowball-like glaciation[1,21,23], occurring during the pan-African orogen. We recently demonstrated that the CO_2 threshold required to initiate a snowball Earth when using the low-to-high latitude continental configuration proposed in ref. 20 is extremely low, around 80 p.p.m. (ref. 26). Furthermore, using the GEOCLIM model, we showed that this palaeogeography leads to restricted CO_2 consumption by silicate weathering (owing to the large percentage of continents located at high latitude), resulting in high steady-state CO_2 (around 1,500 p.p.m.)[26]. Under this atmospheric CO_2 level, GEOCLIM simulates a snow accumulation pattern compatible with a regional scale glaciation occurring over the West Gondwana and the Laurentia cratons, and appears consistent with interpretations made from Varangian data[1,21,23].

In summary, this study provides a well-quantified mechanism to explain the Sturtian glaciation, which was perhaps the most extensive glaciation in the past billion years. We also note that palaeoreconstructions for both younger glacial epochs are highly contentious, and a rigorous application of our model must await further palaeomagnetic data for these events. Furthermore, our study should also be considered as a basis for re-investigating Phanerozoic p_{CO_2} evolution by explicitly taking into account the tectonic forcing factor. More explicit modelling will help to reveal the importance of the tectonic forcing over all the Earth's history. □

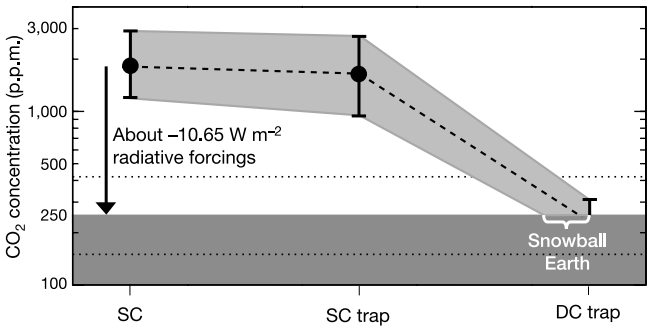

Figure 3 Atmospheric CO_2 history during the time period preceding the Sturtian snowball event. Steady-state atmospheric CO_2 level achieved by the GEOCLIM model for the SC runs, for the SC runs with the inclusion of basaltic provinces (denoted SC trap), and for the DC runs also with basaltic provinces (denoted DC trap). Vertical bars denote the upper and the lower range of atmospheric CO_2 levels calculated using (for the SC runs) a 20% increase and a 20% decrease in degassing flux, and (for the SC trap and DC trap runs) a 20% increase and a basaltic surface of 4×10^6 km^2 and a 20% decrease and a basaltic surface of 8×10^6 km^2 (see Methods). Dark grey area as Fig. 2. The vertical arrow displays the change of the radiative forcing from direct CO_2 effects alone.

Methods

General design of the GEOCLIM model

The COMBINE model is an atmosphere (one reservoir)–ocean (five reservoirs) geochemical model originally coupled to an 1D EBM[10]. Hence, this model incorporates latitudinal variation in temperature, runoff and exposed land area. The improvement of the COMBINE model that we perform here mainly consists in adding the longitudinal dimension to calculate the chemical weathering rates as the climatic variables (temperature and runoff) will now be provided by the CLIMBER-2 model on a 7×18 grid instead of the 1×18 grid of the EBM. The EBM is thus completely removed from the COMBINE code, and is replaced by CLIMBER-2 output. Moreover, the calculated runoff is no longer the result of a parametric law involving the zonally averaged continental surface and air temperature, but is now calculated by the CLIMBER-2 model, which explicitly simulates the hydrologic cycle.

Indirect coupling

A full coupling between COMBINE and CLIMBER-2 cannot be achieved owing to excessive computation times. For both continental configurations, shared boundary conditions include a solar luminosity 6% below the present-day value. In addition, we assume that the Earth's orbit around the Sun was circular (eccentricity = 0) and that the Earth's obliquity was 23.5°. This setting leads to an equal annual insolation for both hemispheres. The land surface in the climate model has the radiative characteristics of a desert and has a uniform elevation of 100 m for both palaeogeographies. Otherwise, the climate model was run until equilibrium (5,000 yr) under an atmospheric CO_2 concentration of 10,000 p.p.m. as an initial condition. Then starting from the previous equilibrium state each time, we conducted a set of simulations (5,000 yr for each to reach equilibrium) in which CO_2 levels were decreased step by step until we reach the CO_2 level for which a global glaciation occurred. More than 40 simulations have been performed in this way in order to have, at least, a climate simulation for each 1 °C of global cooling.

We assume a linear behaviour in between each climatic simulation and thus, by doing a linear interpolation, we obtain the climatic variables of interest (temperature and runoff) for any p_{CO_2} on a 7×18 grid. These climatic parameters allow the calculation of the weathering rates within the 126 grid elements using the weathering law updated in the ref. 13. Fixing the CO_2 degassing to a given constant value, COMBINE is run until a steady-state p_{CO_2} is reached. At each time step of the calculation, temperature and runoff for each grid element are calculated through linear interpolation of the CLIMBER-2 results, for the coeval p_{CO_2} calculated by COMBINE. Because all results are displayed once carbon cycle steady-state is reached (after 4 to 6 simulated million years), the exact kinetics used to describe the various deposition processes as well as the weathering of continental oxidized and reduced sedimentary carbon are not of primary importance for this study, influencing only the response time and behaviour of the model during the steady-state approach. The only two parameters totally defining the steady-state p_{CO_2} are the volcanic CO_2 degassing, and the global continental silicate weathering summed up on each grid cell[12]. An exhaustive description of the COMBINE model is thus not of primary importance for the present study, but can be found in ref. 10.

Regarding the volcanic CO_2 degassing, it might be argued that the break-up of a supercontinent may be characterized by increasing CO_2 degassing flux (via rift-related volcanism), counteracting the global cooling initiated by enhanced weathering. However,

despite the fact that degassing probably increased during the early phase of continental break-up, there is no clear evidence for long-term (10^7-yr timescale) sustained degassing increase. Indeed, no clear consensus exists between the various reconstructions of the degassing flux through the geological past. For instance, recent re-evaluation of ridge production since 180 Myr ago suggests a roughly constant degassing rate since the middle Jurassic[27], in complete disagreement with previous reconstruction[28]. To account for the hypothetical changes in the background degassing flux, we run the model for each continental configuration with values of the degassing flux ranging from a 20% decrease to a 20% increase relative to the present-day value (6.8×10^{12} mol of carbon per year; this is the value required to balance the global consumption through the weathering of silicate lithologies[29]). These choices are somewhat arbitrary, but serve as a reasonable basis for probing the sensitivity of the system (see Figs 2 and 3).

Regarding the global weathering of continental surfaces, we use the most recent field weathering law for granitic lithology[13] to calculate this flux as a function of the air temperature and continental runoff for each grid element. The relative proportion of silicate and carbonate outcrops is assumed to be the same in each grid cell because of the lack of precise lithological control. For the runs accounting for the basaltic provinces, the exact locations of the basaltic surface and the supports for such emplacement are fully described in ref. 8 and are broadly shown in Fig. 1. The total basaltic surface is 6×10^6 km^2 for the standard runs.

Received 7 November 2003; accepted 6 February 2004; doi:10.1038/nature02408.

1. Evans, D. Stratigraphic, geochronological, and paleomagnetic constraints upon the Neoproterozoic climatic paradox. *Am. J. Sci.* **300,** 347–433 (2000).
2. Sohl, L. E., Christie-Blick, N. & Kent, D. V. Paleomagnetic polarity reversals in Marinoan (ca 600 Ma) glacial deposits of Australia: Implications for the duration of low-latitude glaciation in Neoproterozoic time. *Geol. Soc. Am. Bull.* **111,** 1120–1139 (1999).
3. Kirschvink, J. L. in *The Proterozoic Biosphere: A Multidisciplinary Study* (eds Schopf, J. W. & Klein, C. C.) 51–52 (Cambridge Univ. Press, Cambridge, 1992).
4. Hoffman, P. F. & Schrag, D. P. The snowball Earth hypothesis: testing the limits of global change. *Terra Nova* **14,** 129–155 (2002).
5. Hyde, W. T., Crowley, T. J., Baum, S. K. & Peltier, R. W. Neoproterozoic 'snowball Earth' simulations with a coupled climate/ice-sheet model. *Nature* **405,** 425–429 (2000).
6. Donnadieu, Y., Fluteau, F., Ramstein, G., Ritz, C. & Besse, J. Is there a conflict between the Neoproterozoic glacial deposits and the snowball Earth model: an improved understanding with numerical modelings. *Earth Planet. Sci. Lett.* **208,** 101–112 (2003).
7. Schrag, D. P., Berner, R. A., Hoffman, P. F. & Halverson, G. P. On the initiation of a snowball Earth. *Geochem. Geophys. Geosyst.* **3,** 101029/2001GC000219 (2002).
8. Goddéris, Y. *et al.* The Sturtian "snowball" glaciation: fire and ice. *Earth Planet. Sci. Lett.* **211,** 1–12 (2003).
9. Petoukhov, V. *et al.* CLIMBER-2: a climate system model of intermediate complexity. Part I: model description and performance for present climate. *Clim. Dyn.* **16,** 1–17 (2000).
10. Goddéris, Y. & Joachimski, M. M. Global change in the late Devonian: modelling the Frasnian-Famennian short-term carbon isotope excursions. *Palaeogeogr. Palaeoclimatol. Palaeoecol.* **202,** 309–329 (2004).
11. Li, Z. X. *et al.* Geochronology of Neoproterozoic syn-rift magmatism in the Yangtze Craton, South China and correlations with other continents: evidence for a mantle superplume that broke up Rodinia. *Precambr. Res.* **22,** 85–109 (2003).
12. Walker, J. C. G., Hays, P. B. & Kasting, J. F. A negative feedback mechanism for the long-term stabilization of Earth's surface temperature. *J. Geophys. Res.* **86,** 9776–9782 (1981).
13. Oliva, P., Viers, J. & Dupré, B. Chemical weathering in granitic crystalline environments. *Chem. Geol.* **202,** 225–256 (2003).
14. Berner, R. A. The rise of plants and their effect on weathering and atmospheric CO_2. *Science* **276,** 544–546 (1997).
15. Millot, R., Gaillardet, J., Dupré, B. & Allègre, C. J. The global control of silicate weathering rates and the coupling with physical erosion: new insights from rivers of the Canadian Shield. *Earth Planet. Sci. Lett.* **196,** 83–98 (2002).
16. Dessert, C. *et al.* Erosion of Deccan Traps determined by river geochemistry: impact on the global climate and the $^{87}Sr/^{86}Sr$ ratio of seawater. *Earth Planet. Sci. Lett.* **188,** 459–474 (2001).
17. Ganopolski, A., Rahmstorf, S., Petoukhov, V. & Claussen, M. Simulation of modern and glacial climates with a coupled model of intermediate complexity. *Nature* **391,** 351–356 (1998).
18. Donnadieu, Y., Ramstein, G., Fluteau, F., Roche, D. & Ganopolski, A. The impact of atmospheric and oceanic heat transports on the sea ice-albedo instability during the Neoproterozoic. *Clim. Dyn.* (in the press).
19. Meert, J. G. A synopsis of events related to the assembly of eastern Gondwana. *Tectonophysics* **362,** 1–40 (2003).
20. Meert, J. G. & Torsvik, T. H. The making and unmaking of a supercontinent: Rodinia revisited. *Tectonophysics* **375,** 261–288 (2003).
21. Barfod, G. H. *et al.* New Lu-Hf and Pb-Pb constraints on the earliest animal fossils. *Earth Planet. Sci. Lett.* **201,** 203–212 (2002).
22. Knoll, A. H. Learning to tell Neoproterozoic time. *Precambr. Res.* **100,** 3–20 (2000).
23. Rice, A. H. N., Halverson, G. P. & Hoffman, P. F. Three for the Neoproterozoic: Sturtian, Marinoan and Varangerian glaciations. *Geophys. Res. Abstr.* **5,** 11425 (2003).
24. Pisarevsky, S. A., Komissarova, R. A. & Khramov, A. N. New palaeomagnetic result from Vendian red sediments in Cisbaikalia and the problem of the relationship of Siberia and Laurentia in the Vendian. *Geophys. J. Int.* **140,** 598–610 (2000).
25. Trindade, R. I. F., Font, E., D'Agrella-Filho, M. S., Nogueira, A. C. R. & Riccomini, C. Low-latitude and multiple geomagnetic reversals in the Neoproterozoic cap carbonate, Amazon craton. *Terra Nova* **15,** 441–446 (2003).
26. Donnadieu, Y., Goddéris, Y., Ramstein, G. & Fluteau, F. in *Multidisciplinary Studies Exploring Extreme Proterozoic Environment Conditions* (eds Jenkins, G. S., McMenamin, M., McKay, C. P. & Sohl, L. E.) (American Geophysical Union, Washington DC, in the press).
27. Rowley, D. B. Rate of plate creation and destruction: 180 Ma to present. *Geol. Soc. Am. Bull.* **114,** 927–933 (2002).
28. Gaffin, S. Ridge volume dependence on seafloor generation rate and inversion using long term sea level change. *Am. J. Sci.* **287,** 596–611 (1987).
29. Gaillardet, J., Dupré, B., Louvat, P. & Allègre, C. J. Global silicate weathering and CO_2 consumption rates deduced from the chemistry of the large rivers. *Chem. Geol.* **159,** 3–30 (1999).
30. Poulsen, C. J., Pierrehumbert, R. T. & Jacob, R. L. Impact of ocean dynamics on the simulation of the Neoproterozoic "snowball Earth". *Geophys. Res. Lett.* **28,** 1575–1578 (2001).

Competing interests statement The authors declare that they have no competing financial interests.

Correspondence and requests for materials should be addressed to Y.D. (tiphe@lsce.saclay.cea.fr).

Millennial and orbital variations of El Niño/Southern Oscillation and high-latitude climate in the last glacial period

Chris S. M. Turney[1]*, A. Peter Kershaw[2], Steven C. Clemens[3], Nick Branch[4], Patrick T. Moss[5] & L. Keith Fifield[6]

[1]*School of Archaeology and Palaeoecology, Queen's University, Belfast BT7 1NN, UK*
[2]*School of Geography and Environmental Science, Monash University, Victoria 3800, Australia*
[3]*Geological Sciences, Brown University, Providence, Rhode Island 02912-1846, USA*
[4]*Department of Geography, Royal Holloway, University of London, Egham, Surrey TW20 0EX, UK*
[5]*Department of Geography, University of Wisconsin-Madison, 550 N Park Street, Madison, Wisconsin 53706, USA*
[6]*Department of Nuclear Physics, Research School of Physical Sciences and Engineering, Australian National University, Canberra, Australian Capital Territory 0200, Australia*

* Present address: School of Earth and Environmental Sciences, University of Wollongong, Wollongong, New South Wales 2522, Australia

The El Niño/Southern Oscillation (ENSO) phenomenon is believed to have operated continuously over the last glacial–interglacial cycle[1]. ENSO variability has been suggested to be linked to millennial-scale oscillations in North Atlantic climate during that time[2,3], but the proposals disagree on whether increased frequency of El Niño events, the warm phase of ENSO, was linked to North Atlantic warm or cold periods. Here we present a high-resolution record of surface moisture, based on the degree of peat humification and the ratio of sedges to grass, from northern Queensland, Australia, covering the past 45,000 yr. We observe millennial-scale dry periods, indicating periods of frequent El Niño events (summer precipitation declines in El Niño years in northeastern Australia). We find that these dry periods are correlated to the Dansgaard–Oeschger events—millennial-scale warm events in the North Atlantic climate record—although no direct atmospheric connection from the North Atlantic to our site can be invoked. Additionally, we find climatic cycles at a semiprecessional timescale (~11,900 yr). We suggest that climate variations in the tropical Pacific Ocean on millennial as well as orbital timescales, which determined precipitation in northeastern Australia, also exerted an influence on North Atlantic climate through atmospheric and oceanic teleconnections.

Within the North Atlantic region, the last glacial period (60–10 kyr ago) was characterized by a series of rapid millennial-scale climatic oscillations referred to as Dansgaard–Oeschger (D–O) events that have been identified throughout the Northern Hemi-